

Fermi Liquid Properties of a Two Dimensional Electron System

With the Fermi Level Near a van Hove Singularity

D. Menashe and B. Laikhtman

Racah Institute of Physics, Hebrew University, Jerusalem 91904, Israel

We use a diagrammatic approach to study low energy physics of a two dimensional electron system where the Fermi level is near van-Hove singularities in the energy spectrum. We find that in most regions of the ϵ_F - T phase diagram the system behaves as a normal Fermi liquid rather than a marginal Fermi liquid. Particularly, the imaginary part of the self energy is much smaller than the excitation energy, which implies well defined quasiparticle excitations, and single particle properties are only weakly affected by the presence of the van-Hove singularities. The relevance to high temperature superconductivity is also discussed.

Since the discovery of high temperature superconductors (HTSC's), the role played by a saddle point in the energy spectrum, known as a van-Hove singularity (vHS), has been actively debated in the literature [1–8]. The experimental observation of vHS's near the Fermi surface in many HTSC's [8] has led to the so called van-Hove scenario to explain the normal state properties of these materials [3–7], as well as the superconducting properties [1–3]. In this scenario, the presence of the vHS's, as well as weak electron electron (e-e) interactions, are used to explain the main body of experimental data.

One of the more notable properties of the normal state is the linear temperature dependence of the resistivity [8]. This has been explained within the van-Hove scenario by arguing that when the temperature is larger than the energy difference between the Fermi level and the vHS's, the e-e scattering rate is linear in temperature [3–5]. More generally, in this temperature region the imaginary part of the self energy has been claimed to have

the behavior $\text{Im}\Sigma(\mathbf{k}, \epsilon) \propto \max(\epsilon, T)$ for a large range of energies ϵ , thus explaining many other normal state properties [9]. From a theoretical view, the linear energy dependence of $\text{Im}\Sigma(\mathbf{k}, \epsilon)$ differs from the quadratic dependence of a regular Fermi liquid (FL), prompting some workers to classify the system as a marginal Fermi liquid (MFL) [9].

Recently, it has been suggested [7] that the situation is more complicated, and that in a certain region of the ϵ_F - T phase diagram (ϵ_F is relative to the vHS's), FL theory breaks down altogether and a non Fermi liquid (NFL) exists instead. The resulting phase diagram is shown in Fig. 1, and can be summarized as follows: When ϵ_F is small enough, or T is low enough (specific criteria will be given further on), the system behaves as a NFL. In other regions of the phase diagram the system behaves as either a regular FL or a MFL: When $T < |\epsilon_F|$, the affect of the vHS's is not felt and $\text{Im}\Sigma \propto T^2$, indicating a regular FL behavior. In the opposite case the temperature is high enough so that quasiparticles near the Fermi level feel the affect of the vHS's, resulting in the linear temperature dependence of $\text{Im}\Sigma$ characteristic of a MFL.

In the present work we use a standard diagrammatic approach to study the low energy physics of a system of weakly interacting electrons with the Fermi level near vHS's. We show that the leading order perturbation calculation of the self energy [3–5] is invalid, and instead we need to renormalize the self energy by summing diagrams in the particle-particle channel. Dzyaloshinskii [7] used a more complex version of this scheme to show the existence of a NFL in the bottom left corner of the phase diagram in Fig. 1. However, we concentrate rather on the implications for the Fermi liquid properties in the region not occupied by a NFL. For this region, our summation scheme is strictly valid, and our main result is that the energy dependence of $\text{Im}\Sigma(\mathbf{k}, \epsilon)$ is *always* weaker than linear, even in the part of the phase diagram previously thought to contain a MFL. Furthermore, we show that the quasiparticle properties, namely the effective mass and the quasiparticle weight, are only weakly affected by the presence of the vHS's.

These results imply that the van-Hove scenario in it's present form cannot explain fully the normal state properties of HTSC's. These include the linear temperature dependence

of the conductivity [8], the suppression of the quasiparticle weight [9], and the extended nature of most vHS's [8]. Theoretically, the results are important since $\text{Im}\Sigma(\mathbf{k}, \epsilon) \ll \epsilon$, so that quasiparticles are well defined excitations, as required by FL theory. Thus, we conclude that regular FL theory is valid in *all* parts of the phase diagram not occupied by the NFL.

The basic system we discuss here is that of a square lattice with an arbitrary energy spectrum. Due to symmetry, any band of the energy spectrum will have two equal energy saddle points per Brillouin zone (located at wave vectors $(0, \pi/a)$ and $(\pi/a, 0)$, a being the lattice constant). When these points are close to the Fermi level, we shall see that the low energy physics of the system is dominated by electrons occupying regions in \mathbf{k} -space in their vicinity. This enables us to describe the system using the model Hamiltonian

$$H = \sum_{i,\mathbf{k},\sigma} \epsilon_{\mathbf{k}}^{(i)} c_{\mathbf{k},\sigma}^{(i)\dagger} c_{\mathbf{k},\sigma}^{(i)} + \frac{g}{2S} \sum_{i,j,\mathbf{k},\mathbf{k}',\mathbf{q},\sigma,\sigma'} c_{\mathbf{k}+\mathbf{q},\sigma}^{(i)\dagger} c_{\mathbf{k}'-\mathbf{q},\sigma'}^{(j)\dagger} c_{\mathbf{k}',\sigma'}^{(j)} c_{\mathbf{k},\sigma}^{(i)} + \frac{\tilde{g}}{2S} \sum_{i \neq l, t \neq j, \mathbf{k}, \mathbf{k}', \mathbf{q}, \sigma, \sigma'} c_{\mathbf{k}+\mathbf{q},\sigma}^{(i)\dagger} c_{\mathbf{k}'-\mathbf{q},\sigma'}^{(t)\dagger} c_{\mathbf{k}',\sigma'}^{(j)} c_{\mathbf{k},\sigma}^{(l)}. \quad (1)$$

Here S is the sample area, and $c_{\mathbf{k},\sigma}^{(i)\dagger}$ ($c_{\mathbf{k},\sigma}^{(i)}$) creates (annihilates) electrons with spin σ and wave vector \mathbf{k} relative to saddle point i ($= 1, 2$). The spectrum near these points is

$$\epsilon_{\mathbf{k}}^{(1)} = t_x k_x^2 - t_y k_y^2, \quad \epsilon_{\mathbf{k}}^{(2)} = t_y k_x^2 - t_x k_y^2, \quad (2)$$

where $t_x \equiv \hbar^2/2m_x$, $t_y \equiv \hbar^2/2m_y$ and m_x, m_y are the effective masses. If $|t_x - t_y| \ll t_x, t_y$, there is said to be significant nesting between the two saddle point. This is not the general case however, so throughout this work we consider only the non-nested case, meaning $|t_x - t_y| \sim t_x \sim t_y$. g (\tilde{g}) is a \mathbf{k} -independent coupling constant representing processes in which the initial and final saddle points of a given electron are the same (different). Strictly, each of these constants should be split into two, depending on whether or not both incoming electrons are at the same saddle point. However, we will show that only processes where both incoming electrons are at the same saddle point are relevant, thus allowing us to ignore this point. To complete the definition of our model we assume a wave vector cutoff $k_c \sim 1/a$, which defines an energy cutoff $\epsilon_c \sim \max(t_x, t_y) k_c^2$.

To understand the basic physics of this model we first consider a simpler model with only one saddle point instead of two. Thus, we omit the \tilde{g} coupling term in the Hamiltonian, and have only one species of electrons whose spectrum is given by $\epsilon_{\mathbf{k}}^{(1)}$ in Eq. (2). For this model it is convenient to perform a change of variables to $\epsilon_{\mathbf{k}} = tk_x k_y$, where $t \equiv \sqrt{t_x t_y}$. Our original assumption regarding t_x and t_y means that $t \sim t_x, t_y$ and that the new form of the spectrum also has a cutoff $\sim k_c$. The density of states (DOS) for this spectrum is $D(\epsilon) \approx (1/2\pi^2 t) \ln(tk_c^2/\epsilon) \approx (1/2\pi^2 t) \ln(\epsilon_c/\epsilon)$, which diverges at small ϵ , leading to the so called vHS. This means that the main contribution to the DOS comes from states lying close to the saddle point, which justifies our original assumption that the low energy physics is dominated by such states. Furthermore, a simple estimate shows that an electron with energy $\epsilon \ll \epsilon_c$ will typically have a wave vector \mathbf{k} satisfying

$$\ln \frac{k_c}{|k_x|} \sim \ln \frac{k_c}{|k_y|} \sim \ln \frac{\epsilon_c}{|\epsilon|} \gg 1. \quad (3)$$

The above equation, which means that all logarithmic factors appearing in our model are large and of the same order, is central to this work and will be used throughout.

We begin our treatment of the simpler model by considering leading order contributions to $\Sigma(\mathbf{k}, \epsilon)$, which come from the diagrams in Fig. 2a and 2b. When $|\epsilon| < |\epsilon_F|$, it is easy to show that these diagrams give regular FL behavior, meaning $\text{Im}\Sigma \propto \epsilon^2$. Instead, we concentrate on the more interesting case $|\epsilon| > |\epsilon_F|$. Also, for simplicity we neglect finite temperature effects, which serve only to replace ϵ with $\sim T$ when $|\epsilon| < T$. Under these conditions, we obtain

$$\text{Im}\Sigma(\mathbf{k}, \epsilon) = \begin{cases} \frac{-g^2\epsilon}{4\pi^3 t^2} & \text{for } \epsilon = \epsilon_{\mathbf{k}} \\ \frac{-g^2\epsilon}{8\pi^3 t^2} \left(\ln 2 + (1 - \ln 2) \frac{\epsilon_{\mathbf{k}}}{\epsilon} \right) \ln \left(\frac{\epsilon_c}{\epsilon} \right) & \text{for } |\epsilon| \gg |\epsilon_{\mathbf{k}}| \end{cases} \quad (4)$$

The main point here is that the on shell self energy is linear in the energy, which is a signature of MFL behavior. Using the analytic properties of the self energy, we may calculate it's real part. Since this is logarithmically large, it's main contribution is determined by $\text{Im}\Sigma(\mathbf{k}, \epsilon)$ with $|\epsilon| \gg |\epsilon_{\mathbf{k}}|$, so that

$$\text{Re}\Sigma(\mathbf{k}, \epsilon) = \frac{-g^2}{8\pi^4 t^2} [(\ln 2)\epsilon + (1 - \ln 2)\epsilon_{\mathbf{k}}] \ln^2 \left(\frac{\epsilon_c}{\max(|\epsilon_F|, |\epsilon|)} \right). \quad (5)$$

We note that this result is equivalent to that obtained by Dzyaloshinskii [7], who calculated $\text{Re}\Sigma(\mathbf{k}, \epsilon)$ directly. Also, it is a further indication of MFL behavior, since it means that the quasiparticle properties are strongly renormalized in the low energy limit.

We next consider higher order contributions to the self energy. It has been shown [10] that all such contributions may be accounted for by correcting the bare Greens functions of diagrams 2a and 2b, or by replacing one of the interaction lines with a vertex. We will show shortly that corrections to the bare Greens functions are small, thus leaving us with the vertex replacements. The possible vertices are shown in Fig. 2c-2e, and an example of a third order diagram including such vertices is shown in diagram 2f. The singular nature of these vertices has been discussed many times within the context of the van-Hove scenario [1,2,6]. It has been shown that the particle-particle channel has a square logarithmic divergence, i.e. $\Gamma_c \sim t^{-1} g^2 \ln^2(\epsilon_c/\epsilon)$, whereas the particle-hole channel only diverges as a single logarithm, i.e. $\Gamma_d \sim \Gamma_e \sim t^{-1} g^2 \ln(\epsilon_c/\epsilon)$ (here ϵ is the scale of the incoming energies of the vertices, and the subscripts c , d and e refer to Fig. 2). Thus, at low enough energies, we may neglect the particle-hole channel, and need only consider corrections to the self energy coming from the particle-particle channel, Γ_c . Furthermore, for energies such that $(g/t) \ln^2(\epsilon_c/\epsilon) > 1$, these corrections are larger than the leading order contribution to the self energy, thus signaling the breakdown of leading order perturbation theory.

The above arguments can easily be extended to higher order diagrams, which means that the self energy must be renormalized by summing the particle-particle ladder [11] and inserting it into diagrams 2a and 2b, as shown in Fig. 3. For $|\epsilon| < |\epsilon_F|$ we still obtain $\text{Im}\Sigma(\mathbf{k}, \epsilon) \propto \epsilon^2$, however, the important effect of the renormalization can be seen in the opposite case, when $|\epsilon| > |\epsilon_F|$. Here we obtain

$$\text{Im}\Sigma(\mathbf{k}, \epsilon) = \begin{cases} \frac{-g^2\epsilon}{4\pi^3t^2} \left[\frac{1}{1 + (g/8\pi^2t) \ln^2(\epsilon_c/\epsilon)} \right]^2 & \text{for } \epsilon = \epsilon_{\mathbf{k}} \\ \frac{-g\epsilon}{4\pi t} \left(\ln 2 + (1 - \ln 2) \frac{\epsilon_{\mathbf{k}}}{\epsilon} \right) \frac{1}{\ln(\epsilon_c/\epsilon)} & \text{for } |\epsilon| \gg |\epsilon_{\mathbf{k}}| \end{cases} \quad (6)$$

which is the main result of our work. From it, it is clear that as long as $(g/t) \ln^2(\epsilon_c/\epsilon) > 1$, the on shell self energy satisfies $\text{Im}\Sigma(\mathbf{k}, \epsilon) \sim \epsilon/\ln^4(\epsilon_c/\epsilon) \ll \epsilon$. Thus even when $|\epsilon| > |\epsilon_F|$ Landau quasiparticles are well defined, and the system behaves as a regular FL rather than a MFL. Using analyticity, we obtain for the real part of the self energy

$$\text{Re}\Sigma(\mathbf{k}, \epsilon) = \frac{-g}{2\pi^2t} [(\ln 2)\epsilon + (1 - \ln 2)\epsilon_{\mathbf{k}}] \ln \left(\ln \left(\frac{\epsilon_c}{\max(|\epsilon_F|, |\epsilon|)} \right) \right). \quad (7)$$

Comparing to Eq. (5), we see that the real part of the self energy is strongly renormalized, so the affect of the vHS is much weaker then in the leading order case. Using Eq. (7) to calculate corrections to the quasiparticle weight and effective mass, we see they are $\sim (g/t) \ln(\ln(\epsilon_c/\epsilon))$. Since our renormalization procedure is valid for the region $(g/t) \ln^2(\epsilon_c/\epsilon) > 1$, these corrections can generally be considered small. Furthermore, in most samples $|\epsilon_F|$ is finite (see below), so the correction are small even for very low energies. This justifies our not including corrections to the bare Green's function in our renormalization scheme.

However, it is clear that the energy ξ , defined approximately by $(g/t) \ln(\ln(\epsilon_c/\xi)) \sim 1$, is an energy scale below which our approximation becomes invalid. As long as $|\epsilon_F| > \xi$, we may apply our results all the way down to $T = 0$. When $|\epsilon_F| < \xi$, we may assume our results describe the system as long as $T > \xi$. This estimate for the breakdown of our approximation is consistent with the work of Dzyaloshinskii [7]. There, by renormalizing the Greens function in a self consistent manner, it was shown that the quasiparticle weight becomes identically zero at an energy defined by $(g \ln 2/t\pi^2) \ln(\ln(\epsilon_c/\xi)) = 1$. This signifies the onset of the NFL in the bottom left hand corner of Fig. 1. Thus, we conclude that our results remain valid as long as FL theory remains stable, i.e. as long as $\max(T, |\epsilon_F|) > \xi$.

At this point it is instructive to consider typical values of ϵ_c/ϵ for the Cuprates. Since the energy distance of the vHS's from the Fermi level is typically 10 – 20 meV [8], and $\epsilon_c \sim 1$

ev, we obtain $\epsilon_c/|\epsilon_F| \sim 50 - 100$, so the factor $\ln^4(\epsilon_c/\epsilon)$ appearing in the denominator of $\text{Im}\Sigma$ can be as large as ~ 100 . Furthermore, due to the high power of the logarithm, the dependence of $\text{Im}\Sigma$ on ϵ should easily be distinguishable from a linear dependence. Thus, the linear temperature dependence of the resistivity cannot simply be explained by the presence of the vHS's. On the other hand, for the factor $(g/t) \ln(\ln(\epsilon_c/\epsilon))$ appearing in $\text{Re}\Sigma$ to be large, we would need say, $\ln(\ln(\epsilon_c/\epsilon)) > 2$ (assuming weak to intermediate coupling). This in turn means that $\epsilon_c/|\epsilon| > 10^3$, or $|\epsilon| < 1$ meV. Even in samples with very small $|\epsilon_F|$, such an energy scale would probably not be observable due to c-axis coupling, or other smearing mechanisms. Therefore, the presence of the vHS is unlikely to explain the strong renormalization of quasiparticle properties observed in the Cuprates.

Next we consider the full model given by Eq. (1). Besides the intra saddle point processes already discussed, we now include coupling between the saddle points (inter saddle point processes). An example of a leading order inter saddle point contribution to the self energy is shown in Fig. 2g. For the non-nested case we consider here, it can be shown that all such contributions are smaller than the intra saddle point ones discussed earlier [3]. What of higher order inter saddle point contributions, which can be constructed by inserting inter saddle point vertices into diagrams 2a and 2b? Of the various inter saddle point vertices, only the particle-particle vertex shown in Fig. 2h has the necessary $\ln^2(\epsilon_c/\epsilon)$ energy dependence to compete with vertex 2c. Thus, we construct the modified ladder approximation shown in Fig. 4, and obtain for the renormalized scattering vertex

$$\Gamma \approx \frac{g + g^2 a \Lambda^2 + \tilde{g}^2 a \Lambda^2}{1 + g a \Lambda^2 + \tilde{g} a \Lambda^2 + (g a \Lambda^2)^2 - (\tilde{g} a \Lambda^2)^2}, \quad (8)$$

where $\Lambda \equiv \ln(\epsilon_c/\epsilon)$, and $a \equiv 4/((2\pi)^2 t)$. We see that as long as $g > \tilde{g}$ we still have $\Gamma \propto \Lambda^{-2}$ for large Λ , and all our previous results for the self energy remain valid to within prefactors of the logarithmic factors (which now depend on \tilde{g} as well as g). If $g < \tilde{g}$ then the denominator of Eq. (8) becomes zero for large enough Λ , leading to a BCS type instability first pointed out by Gonzalez *et al* [6]. Here we do not dwell on the question of whether or not $g < \tilde{g}$, we merely note that \tilde{g} represents processes with large momentum transfer,

whereas g represents processes with small momentum transfer. Therefore it is reasonable to assume that $g > \tilde{g}$ and that no instability develops.

In conclusion, we have shown that in all regions of the phase diagram where Fermi liquid theory remains valid, the system behave as a regular FL, rather than a MFL. This is based on the fact that $\text{Im}\Sigma(\mathbf{k},\epsilon) \ll \epsilon$ even in the region previously thought to be occupied by a MFL. Furthermore, the effect of the vHS's on the quasiparticle properties, reflected by the real part of the self energy, has been shown to be weak. Our work implies that the van-Hove scenario, in it's present form, cannot explain all the normal state properties of high temperature superconductors.

These results differ not only from the leading order perturbation results [3–5], but also from some more recent attempts to go beyond leading order perturbation theory [6,12]. The renormalization procedure used is strictly valid as long as FL theory remains valid, meaning we are not near the non Fermi liquid region of the phase diagram in Fig. 1. For this region, the more complex theory due to Dzyaloshinskii [7] should be used.

We would like to thank V. Zevin for useful discussions and for reading this manuscript. This research was supported by The S.A. Schonbrunn Research Exndowment Fund.

-
- [1] J.E. Hirsch and D.J. Scalapino, Phys. Rev. Lett. **56**, 2732 (1986).
 - [2] I.E. Dzyaloshinskii, Zh. Eksp. Teor. Fiz. **93**, 1487 (1987) [Sov. Phys. JETP **66**, 848 (1987)];
I.E. Dzyaloshinskii, Zh. Eksp. Teor. Fiz. **94**, 334 (1988) [Sov. Phys. JETP **67**, 844 (1988)].
 - [3] C.C. Tsuei *et al*, Phys. Rev. Lett. **65**, 2724 (1990); C.C. Tsuei *et al*, Phys. Rev. Lett. **69**, 2134 (1992); P.C. Pattnaik *et al*, Phys. Rev. B **45**, 5714 (1992); D.M. Newns *et al* Phys. Rev. Lett. **73**, 1695 (1994); D.M. Newns *et al* Phys. Rev. B **52**, 13611 (1995).
 - [4] P.A Lee and N. Read, Phys. Rev. Lett. **58**, 2691 (1987).
 - [5] S. Gopalan, O. Gunnarson and O.K. Anderson, Phys. Rev. B. **46**, 11798 (1992).
 - [6] J. Gonzalez, F. Guinea and M.A.H. Vozmediano, Europhys. Lett. **34**, 711 (1996); Nucl. Phys. B **485** [FS], 694 (1997).
 - [7] I.E. Dzyaloshinskii, J. Phys. I (France) **6**, 119 (1996).
 - [8] D.H. Lu *et al*, Phys. Rev. Lett. **76**, 4845 (1996) and references therein.; T. Yokoya *et al*, Phys. Rev. Lett. **76**, 3009(1996).
 - [9] C.M. Varma, P.B. Littlewood, S. Schmitt-Rink, E. Abrahams, and A.E. Ruckenstein, Phys. Rev. Lett. **63**, 1996 (1989); Phys. Rev. Lett. **64**, 497 [E] (1990);
 - [10] A.A. Abrikosov, L.P. Gorkov, and I.E. Dzyaloshinski, *Methods of Quantum Field Theory in Statistical Physics*, Prentice-Hall, New Jersey (1963).
 - [11] D. Menashe and B. Laikhtman, Phys. Rev. B **54**, 11561 (1996); H. Fukuyama and Y. Hasegawa, Prog. Theor. Phys. Suppl. **101**, 441 (1990); H. Fukuyama, Y. Hasegawa and O. Narikiyo, J. Phys. Soc. Jpn. **60**, 2013 (1991).
 - [12] W.H. Beere and J.F. Annett, Preprint, cond-mat/9801030 (1998).

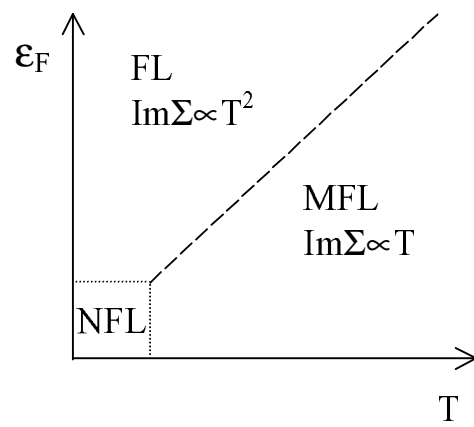
FIG. 1. A schematic phase diagram, as reflected by previous works. Here we show that in the region labeled as a MFL, the system actually behaves as a regular FL. $\epsilon_F = 0$ means that the Fermi level coincides with the energy of the vHS's.

FIG. 2. Diagrams used in this work. Solid (double) lines represent electron propagators near the first (second) saddle point, whereas dashed (double) lines represent g (\tilde{g}) interaction lines. Diagrams (a)-(f) refer to both the full model and the single saddle point model, whereas diagrams (g) and (h) refer only to the full model. (a) and (b) are leading order diagrams for the self energy; (c), (d) and (e) are vertices used to construct higher order self energy diagrams; (f) is an example of such a third order diagram; (g) is an example of a leading order inter saddle point self energy diagram; and (h) is the only inter saddle point vertex which needs to be included in the renormalization of the self energy.

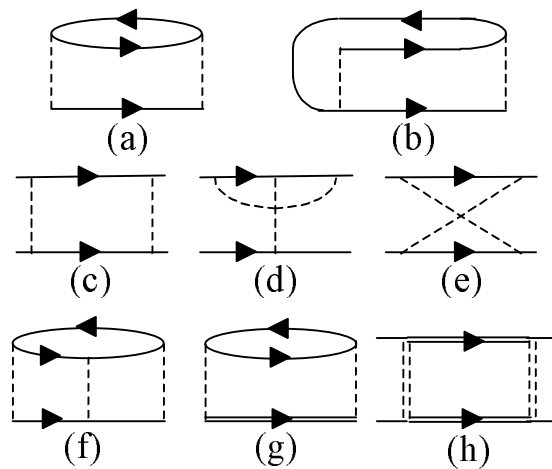
FIG. 3. The ladder approximation for the self energy in the single saddle point model. Γ is the renormalized scattering vertex.

FIG. 4. The ladder approximation for the full model. Γ is the renormalized vertex corresponding to g , whereas $\tilde{\Gamma}$ corresponds to \tilde{g} .

Menashe and Laikhtman - Figure 1



Menashe and Laikhtman - Figure 2

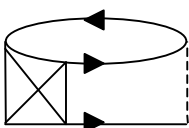
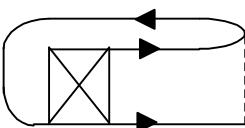


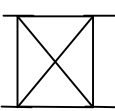

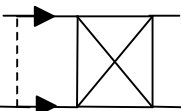
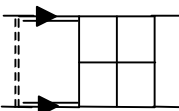
Menashe and Laikhtman - Figure 3

$$\textcircled{\Sigma} = \text{Diagram 1} + \text{Diagram 2}$$

$$\textcircled{\Gamma} \equiv \text{Diagram 3} = \text{Diagram 4} + \text{Diagram 5}$$

Menashe and Laikhtman - Figure 4

$$\textcircled{\Sigma} = \text{Diagram 1} + \text{Diagram 2}$$



$$\textcircled{\Gamma} \equiv \text{Diagram 1} = \text{Diagram 2} + \text{Diagram 3} + \text{Diagram 4}$$





$$\textcircled{\tilde{\Gamma}} \equiv \text{Diagram 1} = \text{Diagram 2} + \text{Diagram 3} + \text{Diagram 4}$$
